URTeC: 2726

NMR Time-Lapse Wettability Assessments in Unconventionals: Insights from Imbibition

S. Kelly[1], R. J. M. Bonnie[1], M. J. Dick[2], D. Veselinovic[2]
[1]ConocoPhillips; [2]Green Imaging Technologies

Abstract

Matrix wettability, the affinity of a fluid to a pore surface, is considered a key driver in recovery factor. In unconventionals, formation wettability and, ultimately, its role in matrix deliverability is often unclear. A robust quantitative method to determine and compare wettability among samples is needed. Such information can potentially influence how operators tailor their completion fluid and enhanced oil recovery strategies. In this study we apply and validate the T_2-based NMR wettability index (NWI) measurement methodology to several sets of twin unconventional samples undergoing oil-displacing-water and water-displacing-oil imbibition to provide a new diagnostic SCAL method: robust and non-destructive time-lapse wettability measurements for tight rocks. This work shows wettability results from two prolific plays, Eagle Ford and Delaware Basin, and covers several key unconventional rock types including marls, chalks, and siltstones.

Introduction

The next frontier of unconventional reservoir (UR) development seeks to optimize existing resources with infilling, remediation, and enhanced oil recovery (EOR) techniques, spawning a multitude of academic studies and vendor offerings in the subject area of fluid-rock interactions. Thus, it is critical to characterize in situ wettability to understand how wettability alteration efforts and fluid tailoring can assist with oil production. Specifically, wettability-determined capillary pressure is an extremely strong force in nanoporous rocks and can act in a fluid transport actuation capacity (counter-current and co-current spontaneous imbibition) as well as a blocking capacity (trapping the nonwetting phase in between menisci often referred to as pendular rings) and/or capillary-end effects [1] at the matrix-fracture interface. Note that a thorough review of wettability fundamentals and capillary pressure for oilfield applications can be found in the work of Hirasaki, 1991 [2].

Classic wettability determination methods that yield quantitative indices include the Amott and USBM methods. These measurements capture changes in saturations with spontaneous and forced imbibition (displacement); a review of these methods and some of their advantages and pitfalls are detailed in [3]. The aforementioned methods have had limited success in tight rocks due to difficulties quantifying saturation changes in the small pore volumes present and the limitations of conventional instrumentation, such as a centrifuge utilized in the USBM test, to reach the pressures required to facilitate incremental forced imbibition (drainage) in nanopores. Rather, Amott cells and modified Amott cells have been utilized in some studies to observe spontaneous imbibition in these rocks [4] and compare differences in uptake rates.

Spontaneous imbibition occurs when a wetting phase spontaneously replaces non-wetting phase(s) due to capillary forces and occurs in porous media and capillary tubes. Many studies, such as [5], have documented that gas (dry) and liquid-saturated tight rocks readily imbibe liquids, often preferential (or sometimes just slightly preferential) to either a water or oil phase; a strong initial imbibition drive dampened with time by viscous forces is not surprising in capillary-pressure driven systems. Preference for both water and oil imbibition can be due to mixed wettability (pore surfaces of varied local wettability), neutral wettability (contact angles closer to 90 degrees), or sample conditions. With respect to the latter, investigators should be cautious that their samples are well preserved and/or re-saturated, as gas (air in ambient tests) supersedes as the nonwetting phase and, ergo, dried or partially dried samples will readily imbibe liquids to fill the gas-filled pore space. Furthermore, investigators should be mindful when seeking to translate results to the field that Amott-style imbibition cell tests have very different boundary conditions than the reservoir and that the extent of co-current and counter-current imbibition is a strong function of said boundary pressures [6]. Particular concerns include that Amott-style imbibition cell tests lack back-pressure and that the enclosed samples have much larger rock surface area to volume ratio than is likely observed at the fracture-matrix interface in the reservoir (save for cases of significant fracturing generating “matrix blocks”). As a result, such tests suggest a wettability state (at the given lab conditions), but do not necessarily represent the in-situ imbibition behavior/rate. The NWI measurement methodology applied to tight rocks in this work provides a quantitative value to enable enhanced comparison between rock samples and varied states: 0.3 to 1 = water wet, -0.3 to 0.3 = mixed wet, and -0.3 to -1 = oil wet. Spontaneous imbibition was utilized in this work as well to generate saturation changes with time; in addition to imbibition rates, temporal changes in saturations and a quantitative wettability index are solved for, as detailed in the subsequent sections.

Samples from two prolific UR plays, Eagle Ford and Delaware Basin, were used in this work such that the methodology was tested on several key unconventional rock types including marls, chalks, and siltstones. Some key sample properties are detailed in Table 1.

Table 1 – Core Plug Sample Information

Rock Type	Sample Name*	Length (cm)	Diameter (cm)	Original State+	Helium Porosity (%)	MICP Porosity (%)	LECO TOC (wt%)	XRD Mineralogy (wt%)	Steady-State NWI**
Chalk	2-P2	5.21	2.58	100% Brine (4% NaCl) Saturated	4.3	4.1	0.39	Quartz: 3.8 Feldspar: 2.3 Carbonate: 85 Total clay: 6.6 Pyrite: 1 Marcasite: 0.7	**0.85 to 0.9 Highly water wet**
	2-P1A	4.59	2.6	100% Decane Saturated					

Marl (organic-rich)	7-P2	4.93	2.61	100% Brine (4% NaCl) Saturated	12.5	12	4.38	Quartz: 21.1 Feldspar: 3.9 Carbonate: 46.5 Total clay: 23.4 Pyrite: 4.6 Marcasite: 0.6	**-0.4 to -0.55** **Fairly oil wet**
	7-P3A	4.97	2.55	100% Decane Saturated					
Siltstone	GP2	5.05	2.53	100% Brine (9% NaCl) Saturated	8.8	8.4	1.89	Quartz: 67.9 Feldspar/ Plagioclase: 6.7 Carbonate: 2.8 Total clay: 14.3 Pyrite: 5.8 Marcasite: 1.6	**0.25 to 0.35** **Mixed wet to slightly water wet**
	GP3	5.07	2.52	100% Decane Saturated					

*Samples for each rock types are twins from the same depth station
***Approximate* steady-state value from convergence of curves from both twin samples
[+] Brine concentrations replicated the corresponding estimated values for formation connate water

Theory and Methods

The work presented in this paper is a continuation of the work presented in our URTEC 2019 paper [7] on applying T_2-based NMR wettability index (NWI) measurement to unconventional samples in order to provide robust wettability measurements for tight rocks. The NWI methodology yields mixing ratios which are then used to compute a wettability index. This work advances the previous study with a larger sample set, prolonged soak times (beyond 100 days), and saturation validation experiments. Specifically, the time-lapse mixing ratios were validated against identical experiments performed with heavy water (D_2O) instead of brine and measured T_1-T_2 maps, enhancing confidence in the robustness of the method. D_2O is invisible to the NMR spectrometer, rendering it ideal for confirming oil saturations during the imbibition process.

The primary objective of this work was to monitor the wettability changes in unconventional samples as a function of time using NMR. This quantification was done by employing the NMR wettability analysis developed by Looyestijn et al. [8,9]; an overview of this method and our implementation of it are detailed in [7] and only a short summary is presented herein. In order to derive an NMR wettability index (NWI), NMR T_2 spectra of (1) 100% brine saturated sample, (2) 100% oil (decane) saturated sample, (3) bulk oil and (4) bulk brine are needed. These spectra are then mixed to give a predicted T_2 spectrum which is compared (via a least-squares fit) to a T_2 spectrum recorded from a sample partially saturated with both water and oil whose wettability is to be determined. See Figure 1 for typical T_2 distributions employed for NMR wettability analysis. All the wettability analysis was carried out in a Matlab routine which read in the T_2 distributions from the NMR data acquisition and analysis software [10].

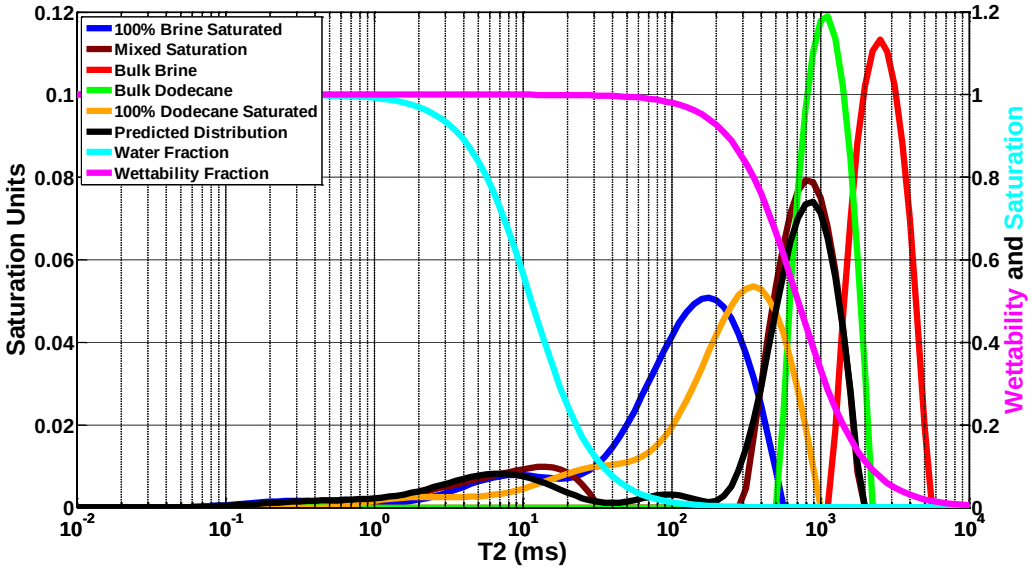

Figure 1: Typical bulk-T_2 spectra used for wettability determination (left axis). The water fraction (light blue) and wettability fraction (pink) are also shown (right axis). This data is for instructional purposes only and was not recorded as part of this investigation of wettability of unconventional samples.

This study expanded our initial data set [7] both in the number of samples investigated and the length of time each sample was monitored for. Table 1 summarizes the physical properties of each 1" diameter core plug sample studied. The samples were comprised of three sets of twins 2-P2/2-P1A, 7-P2/7-P3A and GP2/GP3. For each set of twins, one sample was fully pressure saturated with brine and the other with decane. The twin saturated with decane was then placed into a bath of brine while the twin saturated with brine was placed into a bath of decane. Each sample was left in their baths for increments of time on the order of days while spontaneous imbibition occurred. Data points were obtained when the samples were removed from the baths, their T_2 distributions measured and their wettability and brine saturation determined using the NMR wettability analysis technique. Samples were immediately replaced to their respective baths following a measurement to mitigate drying effects. Such sampling occurred more frequently at early times and at longer time steps as the samples approached equilibrium. Initial data from the 2P and 7P sets of twin samples were presented in our previous work [7]. In this study continuation, the length of time the samples were monitored for was extended from approximately 40 days to over 120 days. The GP twin samples are a new addition to the investigation and also subjected to an extended soak time of 120 days plus.

The NMR T_2 spectra for the wettability analysis were acquired with a GeoSpec NMR spectrometer from Oxford Instruments [11] and Green Imaging Technologies data acquisition and analysis software [10]. The T_2 spectra are measured using a Carr-Purcell-Meibloom-Gill NMR pulse sequence [12] and Table 2 summarizes the NMR parameters employed for this sequence. T_2 spectra for bulk brine and decane were also recorded. Table 2 also summarizes the NMR parameters employed for these scans.

Table 2 – CPMG Parameters.

Sample	Wait Time (TW) (ms)	Signal to Noise Ratio	Tau (µs)	Number of Echoes	NMR Porosity (p.u.) or Volume (ml)	P90 (µs)
2-P2	750	200	50	5000	4.7 p.u.	7.61
2-P1A	750	200	50	5000	4.3 p.u.	7.61
7-P2	3000	200	50	20000	13.7 p.u.	7.61
7-P3A	750	200	50	5000	12.8 p.u.	7.61
GP2	750	200	50	5000	8.3 p.u.	7.61
GP3	750	200	50	5000	7.4 p.u.	7.61
Bulk Decane	18750	164	50	125000	4.69 ml	7.61
Bulk Brine	22500	236	50	150000	6.38 ml	7.61

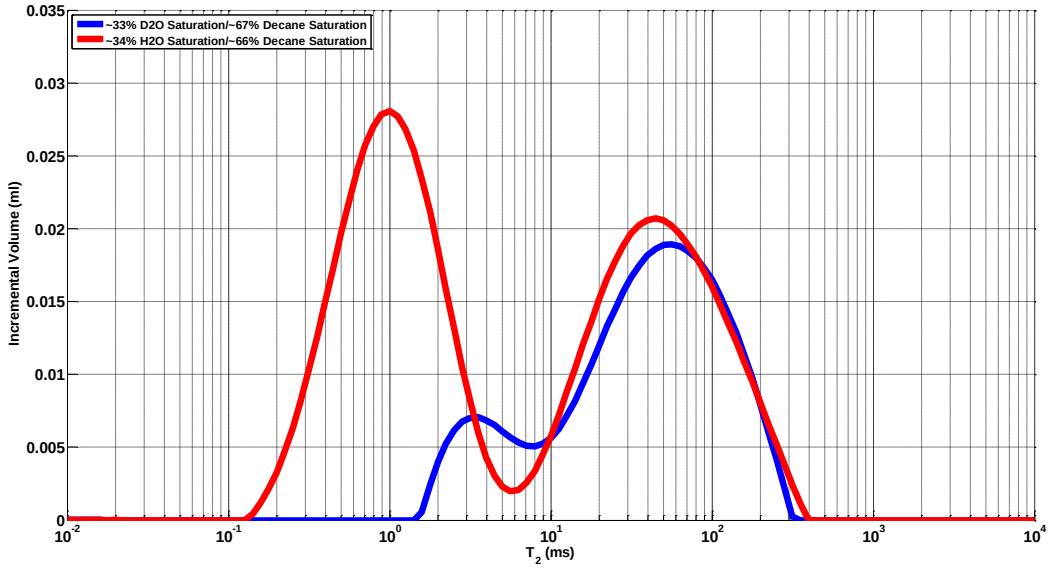

Figure 2: Typical example of T_2 pore size distributions measured with both D_2O (blue trace) and H_2O (red trace) based brines for the same rock at similar saturations. The peak at the lower T_2 values in the H_2O distribution is due to pores filled with water while the peak at higher T_2 values is due to pores filled with decane. The distribution recorded with D_2O based brine only shows the signal from the decane so only the second peak in the distribution is visible.

Additional data with D_2O based brine was also recorded in this investigation to validate the results of the NMR wettability analysis. There is no other wettability method capable of tracking wettability change as a function of time, rendering direct validation of the wettability index impossible. Fortunately, the NMR wettability determination method provides brine saturation as well as the NWI as outputs of the analysis. The brine saturation was verified independently by repeating the imbibition experiments with D_2O based brine in lieu of H_2O based brine. For example, for a sample that was initially 100% decane saturated and allowed to imbibe an H_2O based brine, the experiment was repeated with a rock again fully saturated with decane (care was taken to ensure that respective re-saturated NMR porosities matched the initial experiments) but this time it is allowed to imbibe D_2O based brine. D_2O is "NMR invisible" and, as a

result, only signal from decane in the samples was observed. This approach allowed the saturation of decane (and brine) to be calculated directly. Figure 2 shows a typical example of a T_2 spectrum recorded for the same rock with H_2O based brine versus D_2O based brine. This D_2O based brine saturation can then be compared with the saturation derived from the NMR wettability analysis.

For samples where there is disagreement between the saturation determined from the wettability analysis and the D_2O based saturations, the D_2O based saturations can be employed to fix the brine saturation in the NMR wettability analysis. This calibration allows the wettability prediction method to be repeated and a new NWI determined. The effect on the predicted wettability of the discrepancy, if any, in predicted versus D_2O measured saturation can then be determined.

Results

Chalk Rock Type

Figure 3 shows the results of the wettability analysis for twin samples 2-P1A and 2-P2. Table 1 shows the original state of each twin prior to the initiation of the imbibition experiment. The left-hand panel of Figure 3 displays the wettability as a function of imbibition time for both samples, while the right-hand panel of Figure 3 lists the water saturation as a function of imbibition time for both samples. Looking at the wettability change for twin 2-P1A (Figure 3 – left panel – blue trace), it is observed that the rock started in an oil wet state but changed to water wet within the first 24 hours of brine imbibition. The NMR wettability index then continued to increase until it stabilized around 0.90 at about day five and remained near 0.90 for the duration of the experiment. The brine saturation for twin 2-P1A (Figure 3 – right panel – blue trace) was not as stable. It slowly increased to around 30% by day twenty where it remained stable for the remainder of the experiment. There were some fluctuations in the first five days of the saturation data for sample 2-P1A. Clearly it is not physically possible for a decane saturated rock which is imbibing brine to have its water saturation fluctuate so rapidly. Instead, the instability in the data during the first five days reflects instability in the predictions at early times.

The wettability and saturation levels for sample 2-P2 are also shown in the left and right panels of Figure 3. Looking at the wettability change for twin 2-P2 (Figure 3 – left panel – red trace), it is observed that the rock remained water wet throughout the whole experiment. The brine saturation for twin 2-P2 has not been as stable as the wettability. The saturation slowly changed from near 100% brine saturated to near 90% brine saturated by day forty. Between days forty and sixty there was a precipitative drop in the saturation falling from near 90% brine saturated to near 15% brine saturated where it stabilized for the remainder of the experiment.

Initially it was thought that the aforementioned drop was a result of either sample drying (due to an accidental potential exposure of the top of the sample to air while in its bath) or an issue with the wettability analysis. However, the D_2O saturation data for twin 2-P2 (Figure 3 – right panel – green dots) showed the drop in brine saturation was a real and replicable property of the sample. This drop, though, was not as quick as the wettability analysis had predicted. The D_2O saturation data show that the drop was far more gradual, taking about 120 days before it stabilized near 15%. The discontinuity in the saturation predicted from the wettability analysis is likely due to the active pore-scale capillary changes ongoing within the rock during this period as the systems moves towards an equilibrium. These changes lead to instability in the predictions. As mentioned earlier, similar discontinuities were also observed in the first five days of the

brine saturation data for twin 2-P1A (Figure 3 – right panel – blue trace). The D_2O saturation data for twin 2-P1A (Figure 3 – right panel – black dots) also showed that these oscillations were not real but were likely due to changes occurring within the rock leading to instabilities in the wettability analysis. The D_2O saturation data for twin 2-P1A shows that the brine saturation increased slowly from 0% to between 35-40% by day fifty where it stabilized for the rest of the experiment.

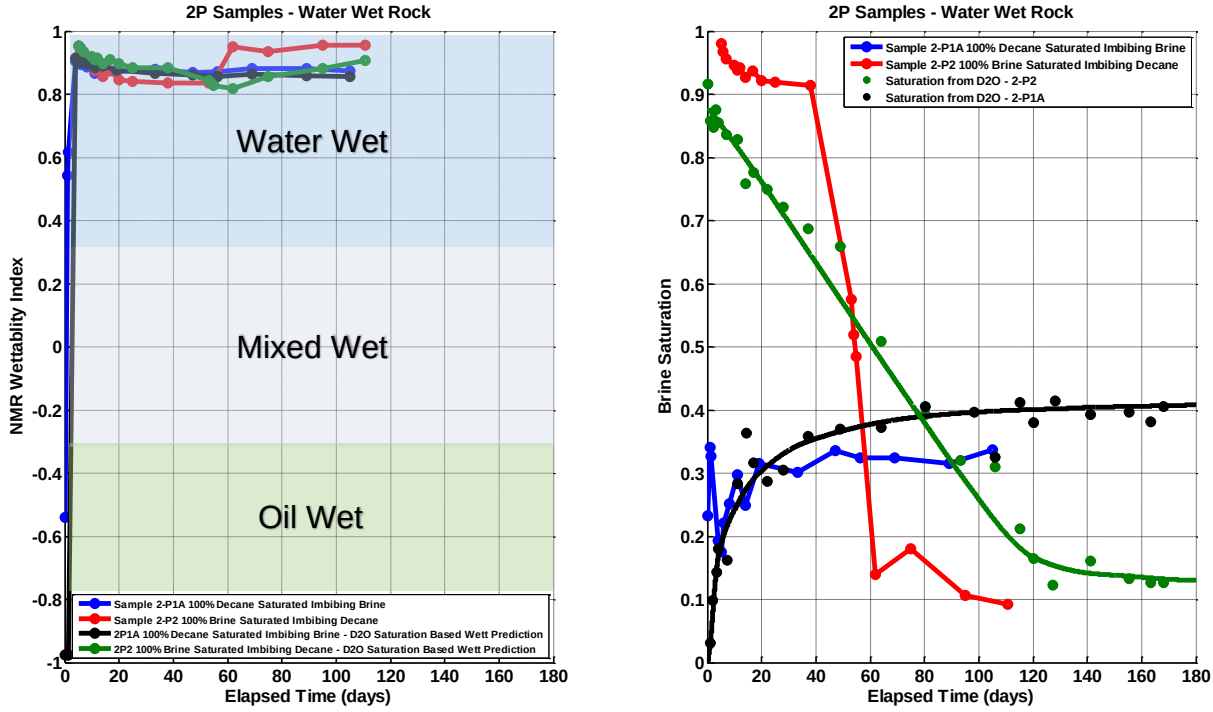

Figure 3: The results of the wettability analyses for twins 2-P1A and 2-P2 are shown. The left-hand panel shows the wettability as a function of imbibition time for both samples, while the right-hand panel shows the water saturation as a function of imbibition time for both samples.

To determine what effect the disagreement between the brine saturation derived from the wettability analysis and the brine saturation determined using D_2O has on the predicted wettability, the T_2 NMR data was reanalyzed. This time the analysis was done with the brine saturation value fixed at the saturation of the 2-P1A and 2-P2 twins as determined from the D_2O data. To accommodate this reanalysis, lines of best fit were drawn through the D_2O data for both the 2-P1A (Figure 3 – right panel – black line) and 2-P2 (Figure 3 – right panel – green line) twins. These fits were then used to calculate the brine saturation based on the D_2O measurement at the corresponding elapsed time for each T_2 NMR wettability measurement made. The green and black traces in the left panel of Figure 3 are the NMR wettability indices calculated with the corresponding D_2O saturation data for twins 2-P2 and 2-P1A. For both twins, the wettability calculated with fixed saturations agrees well with the original wettability prediction, indicating that these samples are highly water wet.

Marl Rock Type

Figure 4 shows the results of the wettability analysis for twins 7-P3A and 7-P2. Table 1 summarizes the original state of each twin prior to the initiation of the spontaneous imbibition experiment. The wettability change for twin 7-P2 (Figure 4 – left panel – red trace) shows that this sample started off water wet and gradually turned to oil wet over time. By day fifty the sample reached an NWI of -0.4 and remained near this wettability for the remainder of the experiment. The wettability change for the twin 7-P3A (Figure 4 – left panel – blue trace) shows that this sample started off very oil wet and slowly became less oil wet as the experiment continued. By day fifty, the wettability of this twin stabilized near -0.55. The brine saturation versus elapsed time data trend for each twin (Figure 4 – right panel) showed a shape similar to its corresponding wettability data. For twin 7-P2, the predicted brine saturation (Figure 4 – right panel – red trace) decreased very quickly dropping from near 100% brine saturated to near 30% brine saturated in the first forty days. The saturation was stable near 30% for the remainder of the experiment. For twin 7-P3A, the predicted brine saturation (Figure 4 – right panel – blue trace) increased quickly in the first ten days increasing from less than 10% to near 20% by day twenty. The saturation remained constant at about 20% for the remainder of the experiment.

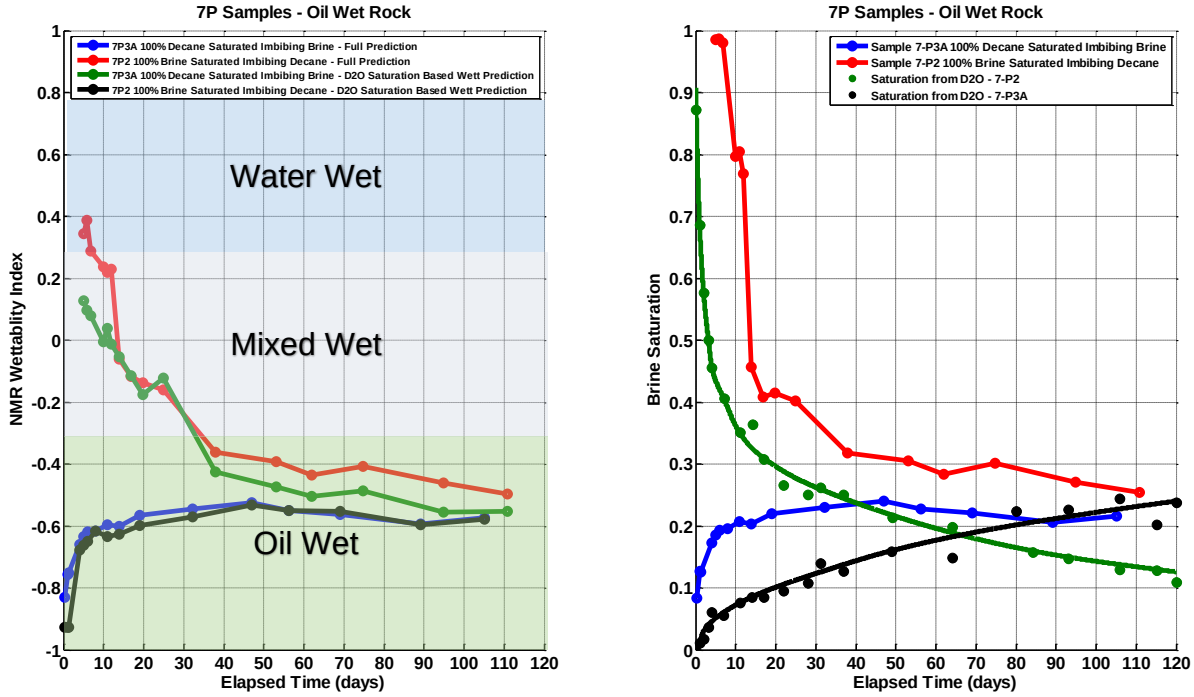

Figure 4: The results of the wettability analyses for twins 7-P3A and 7-P2 are shown. The left-hand panel shows the wettability as a function of imbibition time for both samples, while the right-hand panel shows the water saturation as a function of imbibition time for both samples.

The brine saturation data derived from the D_2O measurements for the 7-P3A/7-P2 twins showed good agreement with the brine saturations predicted by the NMR wettability analysis. As with the brine saturation for twin 7-P2 predicted from the NMR wettability analysis (Figure 4 – right panel – red trace), the saturation based on the D_2O measurements (Figure 4 – right panel – green trace) also dropped very

rapidly during the first forty days from Sw = 100% to circa 20% before slowing for the remainder of the experiment. The final saturation reached based on the D_2O data for twin 7-P2 was about 10% lower than the final saturation predicted from NMR wettability analysis. For twin 7-P3A, the brine saturation as predicted by the D_2O data (Figure 4 – right panel – black trace) showed the same general shape as the brine saturation predicted by the NMR wettability analysis (Figure 4 – right panel – blue trace). However, the brine saturation derived from the D_2O data took longer to reach a stable saturation near 10%.

Despite the reasonably good agreement between the saturations predicted from the wettability analysis and those derived from the D_2O measurements, the wettability for both samples tested were recalculated fixing the saturations at levels computed from the D_2O data. For both twins, the wettability derived with the D_2O based saturations (Figure 4 – left panel – black and blue traces) agreed very well with the wettability derived from the NMR wettability data. All data indicate that these samples are oil wet.

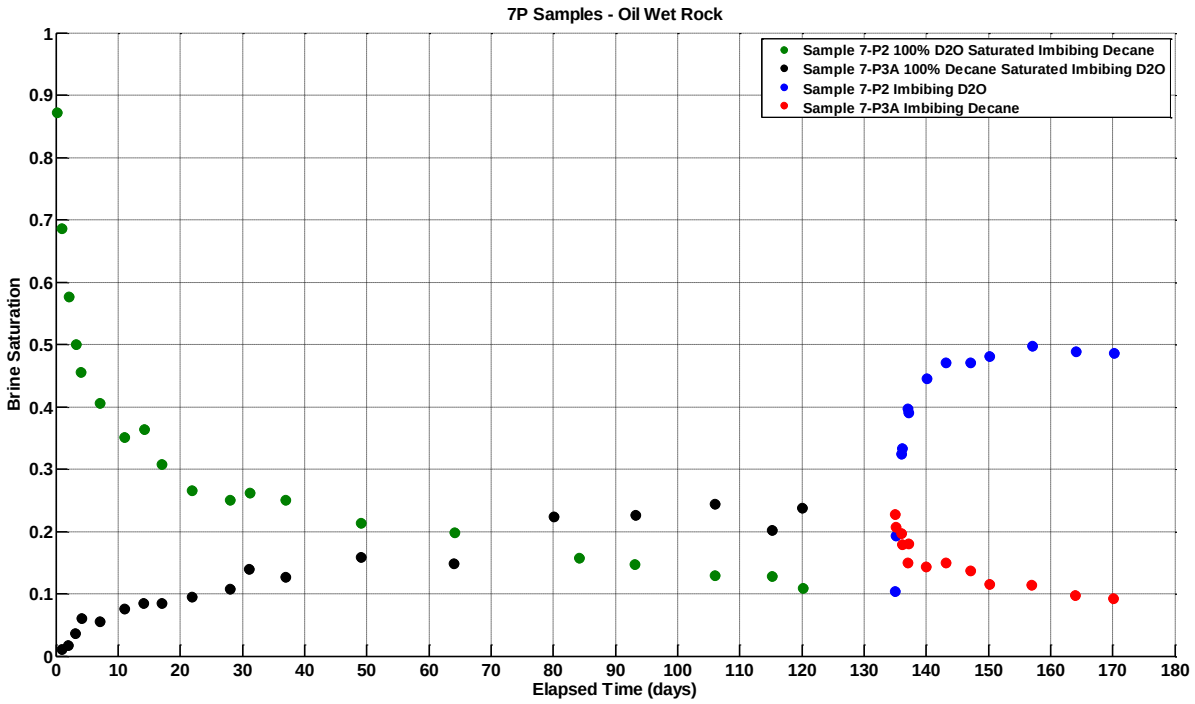

Figure 5: The results of the D_2O saturation analyses for twins 7-P3A and 7-P2 are shown, including saturation reversals to probe imbibition hysteresis.

For twins 7-P2 and 7-P3A, the D_2O experiments continued beyond those plotted in Figure 4. Figure 5 shows the expanded D_2O data set, whereupon hysteresis effects were investigated. Twin 7-P2 was originally 100% D_2O saturated and imbibed decane for the initial 130 days (Figure 5 – green circles) of the experiment. This is the same D_2O based brine saturation data as plotted in the right-hand panel of Figure 4. After day one hundred and thirty, the sample was transferred from its decane bath to one filled with D_2O brine upon which D_2O brine imbibition began (Figure 5 – blue circles). The brine saturation increased, as expected, but did not reach the initial saturation of 100% at the very start of the imbibition experiments. Instead it only recovered to around 50% brine saturation by day 150 and remained near 50% brine saturation

for the remainder of the experiment. Like twin 7-P2, the imbibition of twin 7-P3A was also reversed after day 130. Twin 7-P3A started at 100% decane saturation and had been imbibing D_2O for the 130 days, with brine saturation increasing gradually over this time (Figure 5 – black circles). Again, this is the same data as plotted in the right-hand panel of Figure 4. Following the inversion of the imbibition process after 130 days, the brine saturation in twin 7-P3A was seen to decrease from near 25% and stabilized near 10% by day one 170. As with twin 7-P2, the brine saturation level of twin 7-P3A never returned to its initial value (0%). Clearly there is some hysteresis in these wettability versus elapsed time experiments.

Siltstone Rock Type

Figure 6 shows the results of the wettability analysis for twins GP2 and GP3. Table 1 lists the original state of each twin prior to the initiation of the imbibition experiment. The wettability change for twin GP2 (Figure 6 – left panel – blue trace) shows that this sample started of oil wet and became water wet very quickly within only few days after submersion in water. The wettability change for twin GP3 (Figure 6 – left panel – red trace) shows that sample began very water wet but became less water wet very quickly, also within few days of the experiment. After day 10 the wettability predicted from the NMR analysis had stabilized between 0.2 and 0.4 for both twins. This indicates that the final wetting condition for these samples is slightly water wet. The brine saturation predicted from the NMR wettability analysis for twin GP2 (Figure 6 – right panel – blue trace) showed some oscillations in the first five days. Again, this is attributed to active changes ongoing within the rock during this period leading to instability in the predictions. After five days, the water saturation of sample GP2 stabilized and slowly increased from circa 20% to about 45% by day fifty. The brine saturation predicted by the NMR wettability analysis for sample GP3 (Figure 6 – right panel – red trace) dropped very quickly from near 100% to 70% in the first few days of the experiment. After this initial drop, the rate of brine saturation decreased slowed and eventually stabilized near 60% by day fifty.

The brine saturation data derived from the D_2O measurements for sample GP2 showed good agreement with the brine saturation predicted by the NMR wettability analysis. Both the saturation predicted by the NMR wettability analysis (Figure 6 – right panel – blue trace) and that derived from the D_2O data (Figure 6 – right panel – black trace) increased slowly from 0% to 45% by day 50. The brine saturation then remained more or less constant at 45% for the remainder of the experiment. Agreement between the saturation predicted from the NMR wettability analysis and the D_2O measurements is not as good for sample GP3. The D_2O data (Figure 6 – right panel – green trace) showed a decrease in brine saturation much slower than that derived from the wettability analysis (Figure 6 – right panel – red trace). However, by day fifty the saturations from both assessments show that this plug reached a brine saturation of near 60%. The D_2O analysis continued beyond the length of the NMR wettability analysis for sample GP2. Eventually, the brine saturation derived from the D_2O data stabilized near 50% by day ninety.

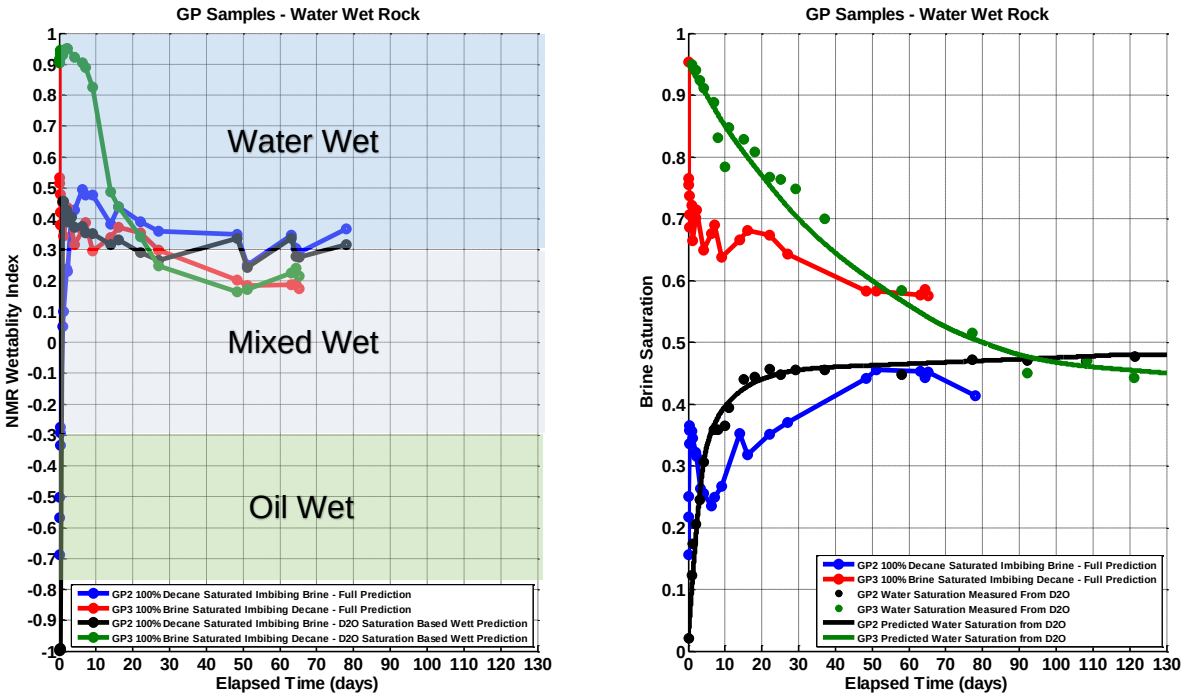

Figure 6: The results of the wettability analysis for twins GP2 and GP3 are shown. The left-hand panel shows the wettability as a function of imbibition time for both samples, while the right-hand panel shows the water saturation as a function of imbibition time for both samples.

As before with the other sets of samples, the brine saturations from the D_2O data were used to fix the saturation in the NMR wettability analysis so that effect of the discrepancies between the brine saturations derived from the NMR data and that derived from the D_2O data can be explored. For twin GP2, the agreement between the wettability derived with the brine saturations derived from the D_2O data (Figure 6 – left panel – black trace) and the wettability derived from the original wettability analysis (Figure 6 – left panel – blue trace) is excellent. Each wettability versus elapsed time plot shows a very rapid increase in wettability from oil wet to slightly water wet in the first few days of the experiment. Following this initial rapid change, the wettability predicted by both methods stabilized near 0.3. For twin GP3, the agreement between the wettability derived from the D_2O data (Figure 6 – left panel – green trace) and that based on NMR wettability analysis (Figure 6 – left panel – red trace) is not as good. The wettability derived from the D_2O data decreased slower than that derived from the NMR wettability analysis with the H_2O based brine. However, both wettability predictions stabilized to near 0.3 by day fifty. All the wettability data recorded for this sample indicates that the sample is slightly water wet.

Discussion

This study rendered serval impactful results. First, the D_2O-oil experiments validate the robustness of the NWI methodology for shales/tight rocks, especially when they converged with the previous brine-oil imbibition results *a priori*. In some cases, improvements to the NWI method fitting were performed *a posteriori* of D_2O data acquisition, a calibration that will likely improve with study scope as various samples and states are tested. Second, the different rock types tested displayed distinct quantitative wettability

differences – i.e., the marl (7-P2/7-P3A) was fairly oil wet, the chalk (2-P2/2-P1A) was highly water wet, and the siltstone (GP-2/GP-3) was slightly water wet. Figure 7 displays the scanning electron microscope images of the corresponding pore systems for these samples – the differences in pore texture among the studied rock types appear to correspond to the NWI results, where the spectrum of pore-lining/pore-filling organic matter (in the monochromatic images, dark gray material is organics, as opposed to black voids and light gray crystalline material) varies from pervasive in the marl, to intermittent in the siltstone, to minimal in the chalk. Revisiting Table 1, we see a similar trend in the organic matter LECO TOC values. Interestingly, a distinctly oil wet state (near a value of -1) was not yet encountered. It is likely that the notable clay and silicate content in the marl and siltstone samples (see mineralogy in Table 1) are hydrophilic surfaces, while the organic matter, intimately associated with carbonate material in the marl samples, is prone to oil-wetness.

The observation that each set of marl and siltstone imbibition saturation curves (Figures 4 and 6, respectively) converged at water saturation values similar to their respective characterized petrophysical in-situ water saturations, regardless of whether brine was displacing oil or vice versa, suggests that any wettability-driven preferential percolation pathways may be associated with separate local pore systems within the rock. Meanwhile, the chalk shows an equilibrium offset between imbibing fluid curves (see Figure 3) and an initially slow saturation change due to decane imbibition (changing only from near 100% brine saturated to near 90% brine saturated by day forty), the latter of which is expected for a highly water wet rock. However, after ~40 days (and sooner in the following D_2O-oil repeat experiment), there is a substantial and swift increase in decane imbibition, which can possibly be explained by the establishment of critical percolation pathways within the samples or a possible increase in sample surface area due to potential microfractures induced during sample handling, In short, these observations suggest that within the chalk samples oil and water are competing within the same pore space with respect to percolation pathways and their imbibition success is highly a function of geometry/connectivity, while the other rock types offer a greater variety of mineral/organic surfaces, such that imbibition is not as limited to key percolation pathways.

In addition, some hysteresis was observed between brine as the invading or displaced fluid cases and when D_2O imbibition was repeated on a sample, suggesting the utility of the NWI method for probing multiple states of the sample. Again, imbibition took place at different rates among the samples before reaching an equilibrium water saturation; this saturation value, or the capacity of the rock to uptake water during spontaneous imbibition, also notably differed among samples and may correspond to pore size and connectivity differences (larger, more well-connected pores promoting swifter imbibition). Differences in open pore spaces between the samples are also seen in the Figure 7 images, though connectivity is challenging to discern from a 2D image. The siltstone and chalk have larger open pore spaces than the marl, but the likely more well-connected siltstone reaches equilibrium considerably faster than the other samples.

Finally, note that any results on core-scale samples submerged in baths or Amott cells may be on the optimistic side for imbibition rates, as the surface area to volume ratio of the sample likely is much higher than that in the reservoir (assuming planar fracture faces). In addition, experiments performed at room temperature, such as the ones in the work, *may* be slightly more oil wet than in the subsurface due to paraffin wax crystallization in the pore space. Nevertheless, the NWI methodology on tight rocks enables a comparative quantitative characterization and is reasonably flexible with respect to the corresponding NMR setup (flow cells, elevated temperature, etc.).

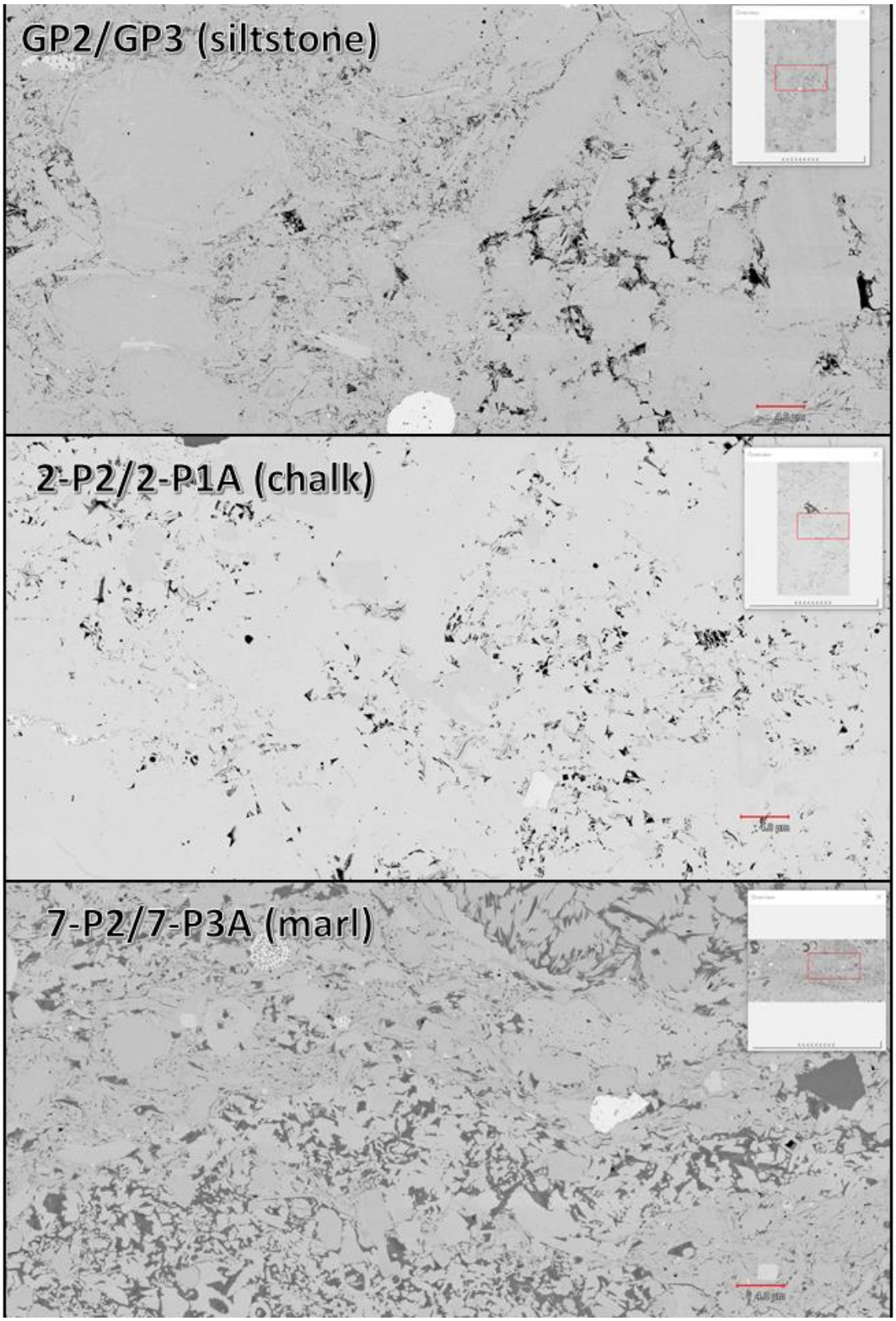

Figure 7: Mosaic BSE-SEM images (5-10 nm/pixel resolution) from the sample depth stations to demonstrate differences in pore texture among the studied rock types, including pore sizes, connectivity, and pore-lining material. All red scale bars (lower right corners) are 4 microns.

Conclusions and Implications

In all, the time-lapse NWI methodology can be used to consistently probe and compare the effects of rock properties, saturations, aging, and injected fluid chemistry (enhanced oil recovery strategies) on wettability alteration. Matrix wettability determines relative permeability, which ultimately impacts recovery factor, especially in the presence of injected water. A robust, repeatable, quantitative method for determining sample wettability and saturation changes is an integration point for petrophysics, geology, geochemistry, and reservoir engineering and can help guide asset team completions fluid decisions with respect to "smart water" or solvent injectates tailored to rock-water surface chemistry.

With respect to practical implications, the long-term nature of this imbibition data set, over 4 months of soak time, renders this dataset interesting to compare with the field-scale, where wells are often subjected to prolonged soak times. In particular, the samples took varied times on the order of days to weeks to reach equilibrium saturation, suggesting a rock type/wettability-dependent time threshold to inform the decision point of how long to soak a well: that is, if a team wishes to reach a particular saturation in the invaded zone (depending on production drive and formation damage mechanisms), then soak to the threshold time, but if wishing to keep the water saturation below a critical value then aim to turn the wells on per the capacity of the rock to uptake water. In addition, the noted hysteresis effects (see Figure 5, for example) should be considered in repeated water injection (including as a mechanism to deliver EOR surfactants) scenarios with respect to the potentially deleterious effect of water blockage.

References

1. G. F. Hadley and L. L. Handy, "A Theoretical and Experimental Study of the Steady State Capillary End Effect," presented at the Fall Meeting of the Petroleum Branch of AIME, 1956.

2. "Wettability: Fundamentals and Surface Forces - OnePetro." [Online]. Available: https://www.onepetro.org/journal-paper/SPE-17367-PA. [Accessed: 04-May-2020].

3. "Characterization of Wettability From Spontaneous Imbibition Measurements - OnePetro." [Online]. Available: https://www.onepetro.org/journal-paper/PETSOC-99-13-49. [Accessed: 04-May-2020].

4. "The Impact of Surfactant Imbibition and Adsorption for Improving Oil Recovery in the Wolfcamp and Eagle Ford Reservoirs - OnePetro." [Online]. Available: https://www.onepetro.org/conference-paper/SPE-187176-MS. [Accessed: 04-May-2020].

5. "Flow-Rate Behavior and Imbibition in Shale - OnePetro." [Online]. Available: https://www.onepetro.org/journal-paper/SPE-138521-PA. [Accessed: 04-May-2020].

6. Q. Meng, H. Liu, and J. Wang, "A critical review on fundamental mechanisms of spontaneous imbibition and the impact of boundary condition, fluid viscosity and wettability," *Advances in Geo-Energy Research*, vol. 1, no. 1, pp. 1–17, Jun. 2017.

7. Dick, M.J., Veselinovic, D., Green, D., Scheffer-Villarreal, A., Bonnie, R.J.M., Kelly, S. and Bower, K. "NMR Wettability Index Measurements on Unconventional Samples", Unconventional Resources Technology Conference, Denver, CO, USA, 22-24 July 2019.

8. Looyestijn, W.J. and Hofman, J.P., "Wettability Index Determination by Nuclear Magnetic Resonance", SPE 93624, presented at the MEOS, Bahrain, March 2005. Published in SPEREE April 2006, pp 146 – 153.

9. Looyestijn, W., Zhang, X., and Hebing, A., "How can NMR assess the wettability of a chalk reservoir", Society of Core Analysts, Vienna, Austria, 27 August-1 September 2017.

10. GIT Systems and LithoMetrix User Manual, Revision 1.9, Green Imaging Technologies.

11. Geo-Spec 2-75 User Manual, Version 1.8, Oxford Instruments.

12. Meiboom, S. and Gill, D., “Modified Spin-Echo Method for Measuring Nuclear Relaxation Times”, Review of Scientific Instruments (1958), 29, 688-691